Recorded ground motion and estimated soil amplification for the May 11, 2011 Lorca earthquake.

Myriam Belvaux, Albert Macau, Sara Figueras, Teresa Susagna, Xavier Goula

EARTHQUAKE SPECTRA

The Professional Journal of the Earthquake Engineering Research Institute

PREPRINT

This preprint is a PDF of a manuscript that has been accepted for publication in *Earthquake Spectra*. It is the final version that was uploaded and approved by the author(s). While the paper has been through the usual rigorous peer review process for the Journal, it has not been copyedited, nor have the figures and tables been modified for final publication. Please also note that the paper may refer to online Appendices that are not yet available.

We have posted this preliminary version of the manuscript online in the interest of making the scientific findings available for distribution and citation as quickly as possible following acceptance. However, readers should be aware that the final, published version will look different from this version and may also have some differences in content.

The DOI for this manuscript and the correct format for citing the paper are given at the top of the online (html) abstract.

Once the final, published version of this paper is posted online, it will replace the preliminary version at the specified DOI.

Recorded ground motion and estimated soil amplification for the May 11, 2011 Lorca earthquake.

Myriam Belvaux,[a] Albert Macau,[b] Sara Figueras,[b] Xavier Goula,[b] and Teresa Susagna[b]

On May 11 2011 an earthquake of magnitude 5.2 (M_w) hit the Murcia region of Spain causing significant damage to buildings in the town of Lorca. Accelerograms were recorded by stations of the Instituto Geográfico Nacional and high-amplitude ground motions were observed at the Lorca station, with a PGA of 0.37g. The contribution of a near-field component of ground motion is shown in time histories and in elastic response spectra. Features of near-field ground motions such as directivity could have significantly enhanced the ground shaking caused by this event. Local amplification effects in Lorca were investigated by the H/V spectral ratio technique and an array method. Information obtained from the geophysical field survey allowed the definition of representative soil columns and site classifications according to Eurocode-8. Modelling of site response is conducted for an example location. The aftershocks recorded at different sites confirm the soil amplification at these locations.

INTRODUCTION

On May 11 2011, a seismic crisis occurred in Lorca, which is situated in the valley of the Guadalentín River, in the region of Murcia, Spain. The 2011 Lorca mainshock (a magnitude M_w 5.2 earthquake at 16:47 UTC) was centered at a shallow depth of about 5 km (relocation obtained by López-Comino *et al*. 2012). The Alhama de Murcia fault was the origin of the earthquake series (Figure 1). Due to the combination of the particularly shallow focus and moderate magnitude, the earthquake resulted in significant shaking throughout the city and the surrounding areas. More specifically in Lorca, the event inflicted substantial damage to its monumental

[a] BRGM, Risks and Prevention Division, 3 Avenue C. Guillemin, BP 36009, 45060 Orléans cedex 2, France
[b] IGC, Institut Geològic de Catalunya, c/ Balmes 209-211, 08006 Barcelona, Spain

architectural heritage and nine deaths were reported. The number of victims was not higher because the population was alerted by an M_w 4.6 foreshock two hours before the mainshock.

Lorca is situated in southeast Spain in the eastern part of the Betic Mountain range, which accommodates the convergence of Africa towards Europe at a rate of 4 to 5 mm/year, with a constant direction since the end of the Miocene (Martínez-Díaz 2002). This convergence is accommodated by deformation within a shear zone oriented NE-SW that distributes seismicity on a zone more than 200 km wide. Displacements along certain segments reach rates of 0.1 to 0.6 mm/year (Masana *et al*. 2004).

The Lorca earthquake occurred in the vicinity of a large active fault system, the Alhama de Murcia fault (AMF), extending over a length of more than 100 km until Alicante, with an inverse-sinistral deformation and a NE-SW direction (Bousquet 1979). It has been an active fault system during the Quaternary period. Paleoseismic studies in the region have established that at least two paleoearthquakes of magnitude larger than 6.5 occurred during the past 30,000 years (Martínez-Díaz *et al*. 2003). Martínez-Díaz *et al*. (2012) studied how strain is accommodated in the intersegment region of the AMF. Mapping recent tectonic structures in the epicentral region, they reveal the structural complexity of this intersegment zone, where the trace of the AMF loses continuity and is characterized by several structures with different dips and orientations.

Even if most earthquakes in the Murcia region are not felt, the region is the location of regular seismic activity, which is related to the AMF. It is worth mentioning earthquakes of 1579 and 1674 with intensities estimated as VII and VIII (EMS-98), which caused significant damage in Lorca (Martínez-Solares and Mezcua 2002). The 1829 earthquake in Torrevieja 100 km east of Lorca (magnitude estimated at 6.3) caused the death of 400 people and destroyed 3,000 houses (Muñoz and Udías 1991). In the region of Murcia, another damaging earthquake occurred near the town of Mula, 45 km to the NE of Lorca, on February 2 1999. Its magnitude was M_w 5.1 (Buforn *et al*. 2005) and according to IGN (1999) the maximum intensity reached a value of VI (EMS-98). Two earthquakes, M_w4.7 in 2002 and M_w5.1 in 2005 (Buforn *et al*. 2005, 2006) occurred to the southwest of Bullas, with some damage to constructions, but fortunately no victims (Gaspar-Escribano *et al*. 2008). It should be pointed out that the Lorca event on May 11 2011 is the first one during the instrumental period that has caused human deaths at the region.

This paper summarizes field observations made by the Spanish Association of Earthquake Engineering (AEIS) together with the Earthquake Engineering Associations of France (AFPS) and Portugal (SPES), (AFPS, 2011; IGC, 2011; IGME, 2011). It presents their findings, firstly on strong ground motion issues and secondly on soil amplification features.

THE LORCA SEISMIC SEQUENCE

The magnitude 5.2 (M_w) mainshock occurred on May 11 2011 at 16:47 UTC about 5 km north of Lorca, at a shallow focal depth of 5 km. The earthquake is estimated to be the direct result of strike-slip-reverse faulting on the AMF system, along a shallow segment 4 km long.

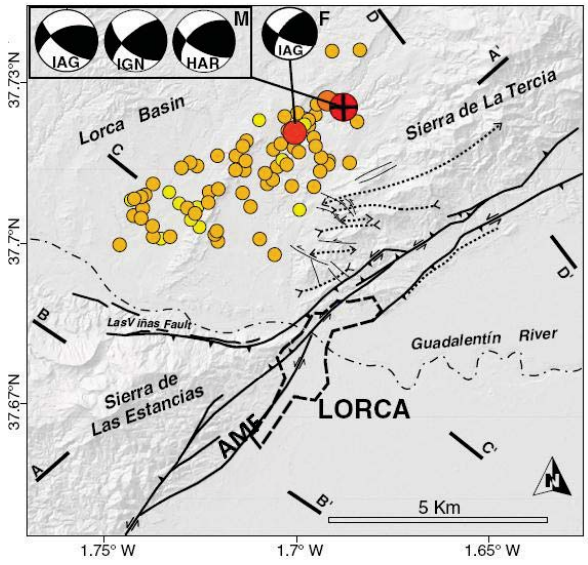

Figure 1. Map of relocated instrumental epicenters of the Lorca sequence until July 7 2011, with the focal mechanism of the foreshock and the mainshock. AMF: Alhama de Murcia fault. (Modified from Martínez-Díaz *et al*. 2012 and López-Comino *et al*. 2012).

This earthquake was preceded two hours before by a magnitude 4.6 (M_w) foreshock that struck very close to the mainshock epicentre at 15:05 UTC. It was located along the same AMF zone, with a similar focal mechanism to the main shock. Though this foreshock was relatively small, some cracks and crumbled walls were reported in Lorca.

The Lorca earthquake was followed by a short aftershock sequence, the strongest reaching a magnitude of 3.9 (M_w) and occurring at 20:37 UTC. The seismic sequence was recorded at 25 broadband seismic stations of the Instituto Andaluz de Geofísica (IAG) and Instituto Geográfico Nacional (IGN) permanent networks within 250 km (epicentral) distance. About a hundred events were detected in the first week. Near-real-time locations by IGN at first showed a diffuse cloud of

aftershocks in the Guadalentín basin, not allowing any spatial trend or link with the AMF to be made. Relocated aftershock locations using IGN and IAG data (Figure 1) show an epicenter distribution that moves significantly towards the mainshock at a distance of about 5 km north of Lorca (López-Comino *et al*. 2012) located to the north of the northern segment of the AMF.

Several authors (Frontera *et al*. 2012, López-Comino *et al*. 2012, Martínez-Díaz *et al*. 2012, Santoyo, 2013) combined radar interferometry with seismological observations of the Lorca seismic sequence to model the earthquake source. Proposed source models suggest that the Lorca earthquake ruptured an area of about 4 by 3 km along a reverse strike-slip fault segment.

The main shock was widely perceived by the population in a wide zone around the epicenter. Determinations of macroseismic intensities were realized by IGN (www.ign.es). Many observations are available for intensities lower or equal to V. For higher intensities, little information is available; only the maximum felt intensity of VII has been reported in Lorca. Figure 2 shows the estimated macroseismic intensities (EMS-98[1]) in adjacent municipalities

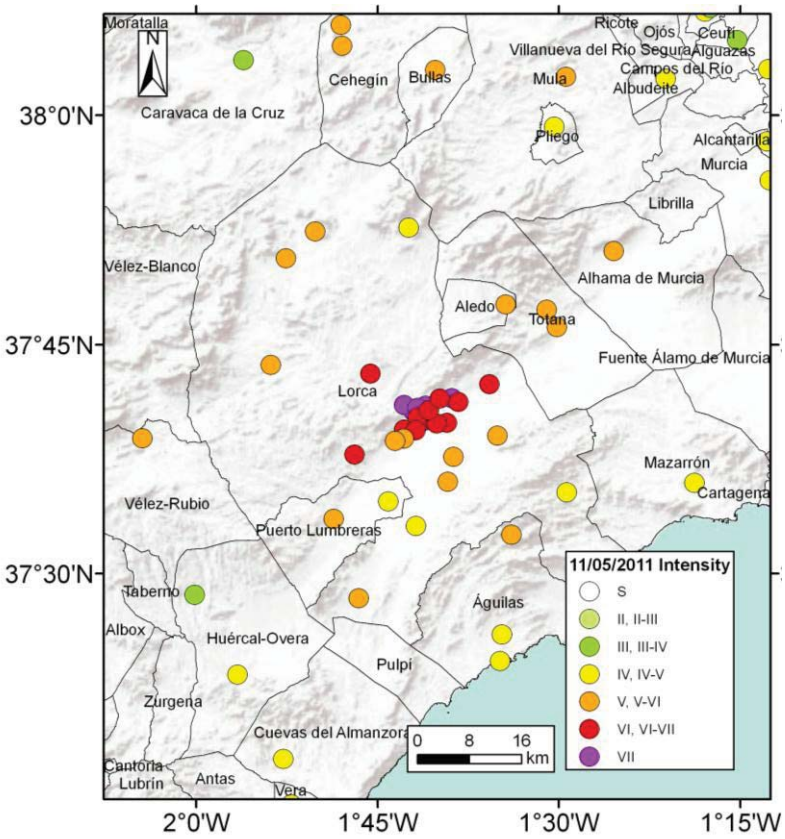

Figure 2. EMS-98 intensity map of the May 11, 2011 mainshock (source IGN).

[1] Intensities up to VII in EMS-98 are equivalent to MM intensities (Musson *et al*. 2010).

where accelerometric records are also available. This information helps in establishing correlations with parameters of engineering interest, especially for moderate magnitude earthquakes, which have been rare since the establishment of seismological networks in Spain.

STRONG MOTION RECORDINGS OF THE LORCA EARTHQUAKE

Within this seismic sequence, 13 earthquakes were recorded by the IGN accelerometric network including the mainshock, the foreshock, and the largest aftershock.

The foreshock (May 11 15:05 UTC; M_w= 4.6) was recorded by five accelerometers, at epicentral distances between 5 and 40 km. The main shock (May 11 16:47 UTC; M_w= 5.2) was recorded by 17 stations located at distances between 6 and 185 km. The largest aftershock (May 11 20:37 UTC; M_w= 3.9) was recorded by four stations at distances between 6 and 39 km. Accelerograms from other aftershocks, all with magnitudes lower than 3.0, were only recorded at the Lorca station (IGN, 2011). Figure 3 shows the location of the IGN accelerometric stations and the horizontal peak ground accelerations (PGAs) recorded during the mainshock. Table 1 presents PGAs and peak ground velocities (PGVs) for each component of the mainshock ground motion obtained on stations that recorded the three previously mentioned earthquakes.

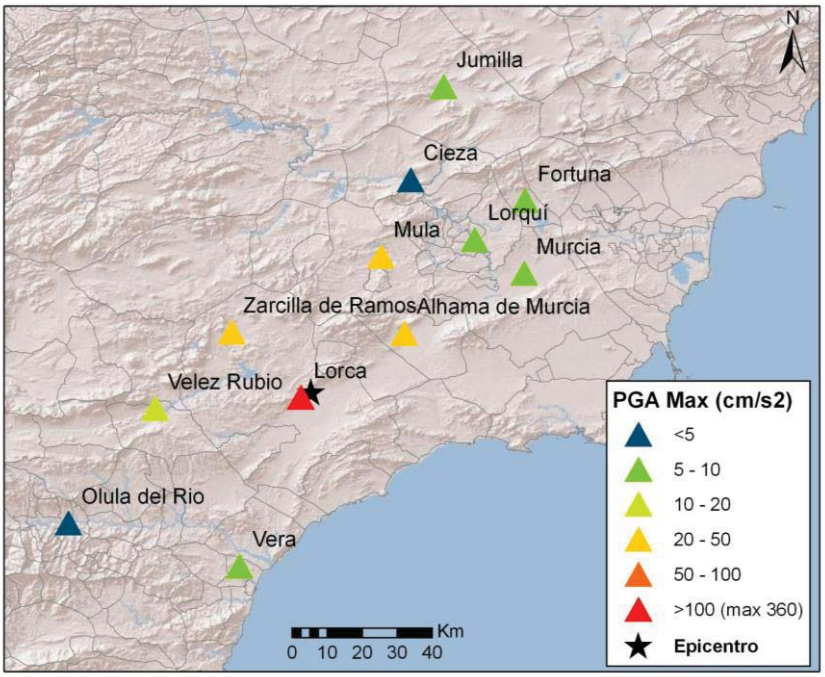

Figure 3. Map of the IGN strong motion stations at distances less than 100 km from the epicentre. PGA values recorded during the Lorca main shock are represented with colors (from Susagna *et al*. 2012).

Table 1. PGA and PGV for the 5 recordings with PGA > 10 cm/s^2 (three components) obtained during the Lorca mainshock.

Station	dist (km)	Comp.	PGA (cm/s^2)	PGV (cm/s)
LORCA	6	E30°N	151.2	14.4
		N30°W	359.5	35.8
		Z	114.2	7.6
ZARCILLA DE RAMOS	21	E	32.0	2.1
		N	25.4	2.2
		Z	26.2	1.3
ALHAMA DE MURCIA	26	E	44.1	2.1
		N	41.0	1.3
		Z	23.5	0.8
VELEZ RUBIO	35	E	9.3	0.6
		N	10.7	0.5
		Z	5.9	0.4
MULA	39	E	41.6	1.4
		N	35.5	1.5
		Z	20.2	0.9

WAVEFORM CHARACTERISTICS IN THE TIME DOMAIN

The PGAs recorded at the Lorca station (LOR) during the first two earthquakes (270 and 360 cm/s^2), are the largest ever detected by instruments on the Iberian Peninsula. This IGN accelerometer is placed in the basement of the former jail, in the elevated part of the ancient town, where conglomerate outcrops are apparent. In consequence, geological features beneath LOR may be considered type A (rock) according to Eurocode 8 (EC8; CEN 2004), even if precise geotechnical data are not available. These high PGAs are mostly due to the proximity to the hypocenter, i.e. a small epicentral distance (about 5 km) and a shallow depth (5 km).

Standard correction process has been applied to all accelerograms (baseline and 0.1Hz highpass filter), except for the Lorca station recordings, which have been highpass filtered with a cut-off of 0.06Hz.

Figure 4 illustrates the dependence of horizontal PGA recorded during the mainshock with epicentral distance. Ground motion prediction equations (GMPEs) derived from PGAs recorded in Europe and the Middle East, are comparable for distances between 20 and 100 km. However, for distances less than 10 km, epistemic uncertainty in the median predicted PGA is higher than a factor of 10 (between 0.1 and 1 g), mainly due to effect of the hypocentral depth as reflected by the curve of Tapia *et al.* (2007) for a depth of 5 km. This shows that for small source-to-site distances (5 km or less), the predicted levels of ground motion are very strongly dependent on the

focal depth of the earthquake.

The curve proposed by Akkar and Bommer (2010) is generally above the other GMPEs, probably because it was adjusted to ground motions from larger earthquakes than the relations developed for Spain, which used data from earthquakes with magnitudes lower than 6. On Figure 4, the points corresponding to the LOR station have been represented at an epicentral distance of 5 km; they could be placed at shorter distances if we consider the rupture dimensions and compute the distance to the surface projection of the rupture (Joyner-Boore distance).

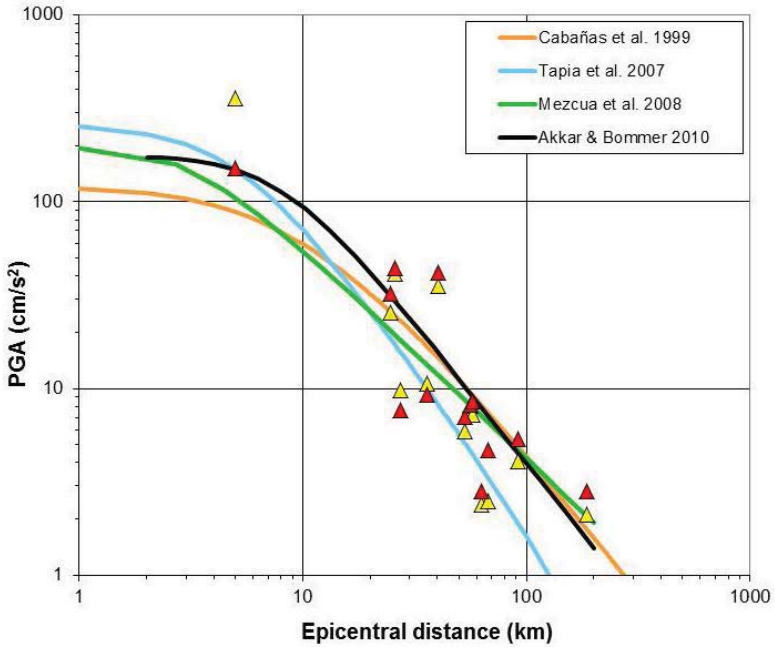

Figure 4. Recorded PGA values from the IGN network with respect to epicentral distance (red triangles for EW components, yellow triangles for NS components) and compared to four GMPEs (Cabañas *et al*. 1999, Tapia *et al*. 2007, Mezcua *et al*. 2008, Akkar & Bommer 2010) for PGA horizontal values.

Based on the IGN macroseismic maps, Susagna *et al.* (2012) compared observed intensities with ground-motion parameters calculated from the recorded accelerograms: PGA, Arias intensity (AI) and cumulative absolute velocity (CAV), which are of interest to the earthquake engineering community. Note that this study used the definition of CAV proposed by EPRI (1991) and called CAV_{STD} (standardized). A value of 0.16 g·s for CAV_{STD} is still used in the nuclear industry (EPRI, 2006) as a (conservative) threshold of damage and, therefore, as a threshold of basic safety. The CAV_{STD} calculated from the horizontal components of LOR accelerograms equal 0.11 g·s and 0.22 g·s. It is the first time that such values have been detected in Spain. Also from published relations between intensity and PGA (Wald *et al*. 1999, Souriau,

2006), intensity VII corresponds to a PGA of 0.07g to 0.23g. Given the expression of intensity as a whole number without decimal, and the inherent scatter in such relations, an intensity VII and the recorded PGAs do not seem to be in conflict with the above-mentioned correlations.

Records obtained at LOR allow analysis of near-field ground motions for an epicentral distance of roughly 5 km. Figure 5 presents the three components of acceleration, velocity and displacement for the main shock recorded at LOR; corresponding maximum values are listed in Table 1. The major part of the energy is liberated in a time interval of about 1 s in three principal pulses. As shown in Figure 5, the maximum displacement observed on the N30ºW component is at least 3 cm (the filtering of the acceleration record may have eliminated part of the actual displacement). The observed motion is constituted of a symmetrical pulse of about 1 s duration.

Attention is focused on the great difference between maximum values recorded in the two horizontal directions. It happens that the LOR sensor orientation, azimuth N30ºW, is almost perpendicular to the fault rupture direction. The large displacement observed on this component is probably linked to a directivity effect, caused by the propagation of the rupture towards Lorca's town center in conjunction with short hypocentral distance. The directivity phenomenon during

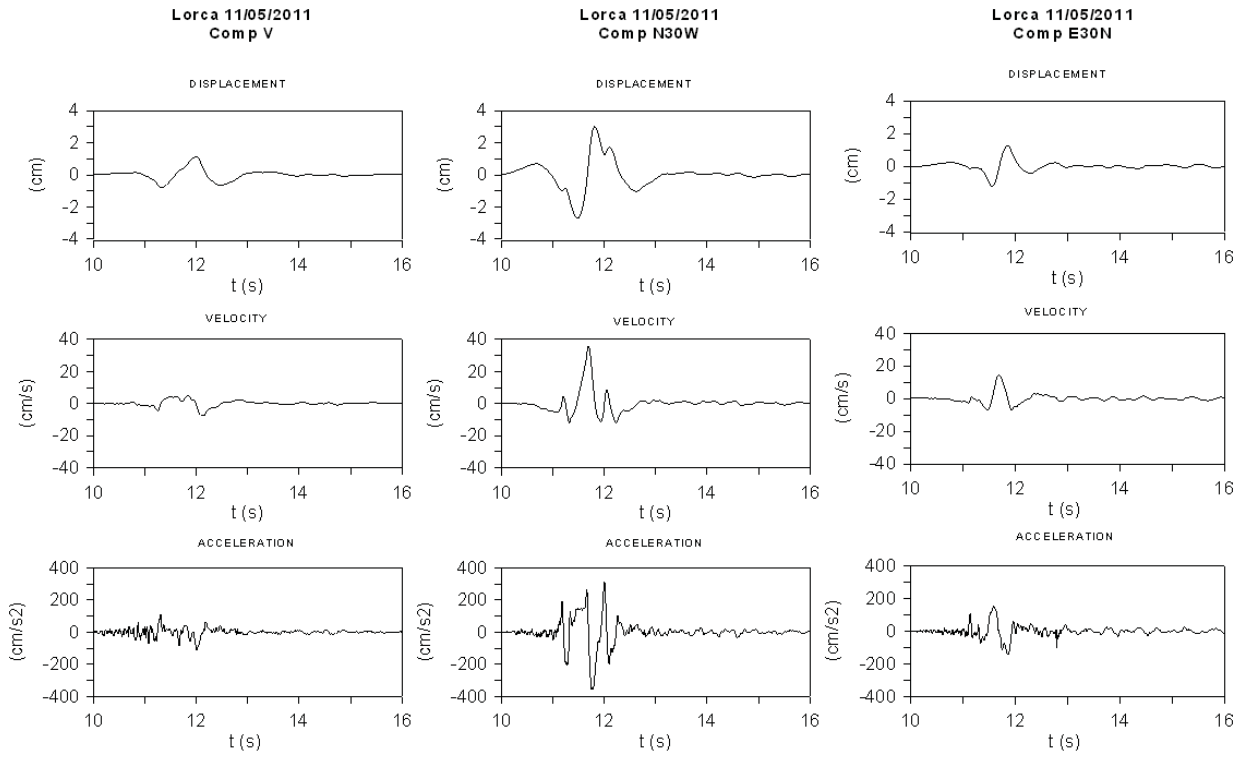

Figure 5. Three-component recordings of the corrected acceleration, velocity and displacement traces of the main shock recorded by the LOR station.

this earthquake is discussed in a subsequent section of the paper.

It was possible to observe the effect of this dynamic horizontal displacement on several buildings and heavy machinery (IGC 2011). It is also worth mentioning that a permanent displacement of a few millimeters has been found for a GPS station located in Lorca (Frontera *et al*. 2012). Residual displacement of some millimeters for the N30ºW channel has been confirmed by Cabañas *et al*. (2013) using sophisticated accelerogram processing.

WAVEFORM CHARACTERISTICS IN THE FREQUENCY DOMAIN

The PGA of 0.37g recorded at LOR is three times larger than the basic acceleration value given for Lorca in the Spanish Seismic Resistant Building Code (NCSE-02) a_b = 0.12g. Figure 6 represents 5%-damping response spectral accelerations for all three components, together with the type 2 EC-8 spectrum for a soil class A scaled to a PGA of 0.37g.

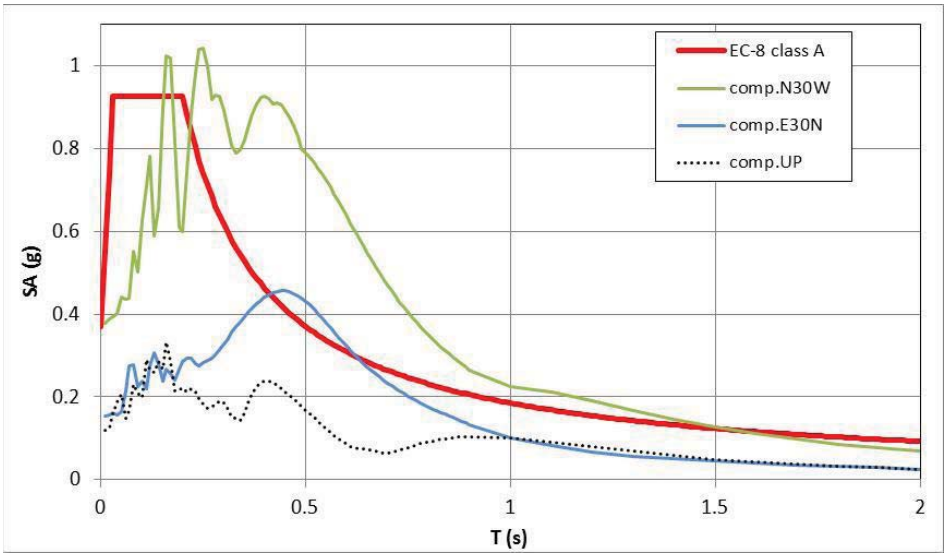

Figure 6. Comparison of EC8 Type 2 acceleration response spectra scaled to PGA of 0.37 g with the spectra from the recorded horizontal ground motion at the LOR station (5 km from the source).

The following remarks can be made: (i) the EC-8 spectral shape fits the observed response spectrum in the short period domain, but the EC-8 plateau is narrower than the observed one; and (ii) a pulse around 0.4 s clearly appears in all three recorded components, which could be due to the influence of the near-field effects, as discussed in the next section.

Near-field recordings of the Chi-Chi earthquake 1999 in Taiwan resulted in exceptionally high spectral ordinates (Chai *et al*. 2000). These authors proposed modifications to the spectral

shapes in the Taiwan code through three amplification factors: at short periods (PGA), for intermediate periods (plateau) and for long periods. They also widen the plateau of the design spectrum. In the case of Lorca, amplifications have been observed in the short periods with a PGA of 0.37g, in the intermediate periods and clearly in the plateau width (Figure 6). On the other hand, no amplification is noticed for long periods, since the spectrum coincides with the type 2 EC-8 spectral shape between 1 and 2 s.

The Uniform Building Code (1997) considers the vicinity of an active fault by means of two near-source amplification factors, Na and Nv, applied respectively to the short and intermediate periods of the acceleration response spectrum. These coefficients, similar to ones proposed for Taiwan, are specified only in high seismicity zones, for distances shorter than 15 km and for three types of fault. Modified seismic design spectra for sites near an active fault aim to increase the seismic capacity of buildings against near-fault ground motions.

DIRECTIVITY EFFECTS

When it appears, the directivity phenomenon especially affects the ground motion in the horizontal directions perpendicular to the fault (Somerville *et al*. 1997, Somerville 2003). Indeed, the radiation diagram of a shear dislocation on a fault produces a wider pulse in the perpendicular direction to the fault plane. For periods longer than roughly 0.5 s, the component parallel to the strike of the fault will thus record a weaker ground motion than the perpendicular component. So for a strike-slip mechanism, directivity appears on the component perpendicular to the fault trace, on sites close to the fault, but also at stations at significant epicentral distances. For dip-slip mechanisms, the alignment of both the rupture direction and the up-dip slip direction produces rupture directivity effects at sites located around the surface expression of the fault.

The segment of the AMF that broke during Lorca earthquake has a N60ºE azimuth, and corresponds to strike-slip-reverse faulting on a fault plane dipping 55° - 70° northward; the rupture mainly propagated from east to west and from depth to the ground surface. Indeed, polarization was observed in the ground motions recorded at LOR, the N30ºW component showing higher values of PGA, PGV and spectral ordinates than the N60ºE component.

The presence of a clear pulse at 0.4 s on all three components of the LOR response spectra could be caused by the same directivity phenomenon. The period of the directivity pulse generally increases with magnitude, since it is linked to the dislocation rise time and to the fault

dimensions, which both increase with magnitude. For a magnitude 6 event, the pulse period is close to 0.8 s. It can increase to 4 s for a 7.5 magnitude earthquake (Somerville 2003). For the 2011 Lorca main shock (M_w5.2), the observation of a 0.4 s period pulse is compatible with this trend. The situation of the station in the elevated part of the ancient town and the geological conditions of the site, with apparent conglomerate outcrops make it difficult to find an explanation for the pulse based on soil amplification.

Bommer *et al*. (2001) cite examples of small-to-moderate magnitude earthquakes that caused significant building damage. Among them, a parallel can be found with observations during the 1986 San Salvador earthquake (M_S5.4, M_w5.7). From the analysis of near-field accelerograms, it appears that rupture directivity effects could have played an important role in generating the high ground motions and corresponding spectral ordinates recorded during this earthquake.

Since the first conclusions of the field survey conducted in the epicentral area (AFPS 2011, IGC 2011), evidence of rupture directivity was presented in three recent publications. By processing the LOR strong ground motion records using the wavelet transform, Rueda *et al*. (2011) extracted a directivity pulse with a period of 0.67 s from the seismograms. Their following two analyses (normalized source-time functions resulting from an empirical-Green-function deconvolution and normalized short-period amplitude ratios) confirmed the directivity effect in the NE-SW direction. Based on the relocation of aftershocks recorded using a dense seismic station network, López-Comino *et al*. (2012) computed the seismic moments and focal mechanisms of these aftershocks, and obtained an asymmetric bilateral rupture of the mainshock, with 70% of the rupture propagating in the SW direction. Martínez-Díaz *et al*. (2012) confirmed that the rupture process during the Lorca earthquake clearly caused directivity in the ground motions at Lorca.

SOIL AMPLIFICATION CHARACTERIZATION

Causes of damage to buildings should be investigated considering the local seismic amplification effects arising from the lithostratigraphic and morphological characteristics of the underlying geological formations.

Geological features of Lorca were collected from previous studies. At the scale of interest (1:25,000) pre-existing data are poor (Navarro *et al*. 2008, Navarro *et al*. 2012), leading to a basic classification of prevailing geological formations. In summary, the western part of the town,

where the historical center is located on the buttresses of the castle, is founded on Paleozoic rock outcrops. Towards the north-east, Miocene materials (marls and conglomerates) predominate. The rest of the town is located on soils formed by quaternary soft rocks of the Pleistocene (Glacis), while the eastern zone, the modern part of the town, is situated on recent colluvial and alluvial deposits (Figure 7). The sediment thickness tends to increase towards the basin of the Guadalentín River.

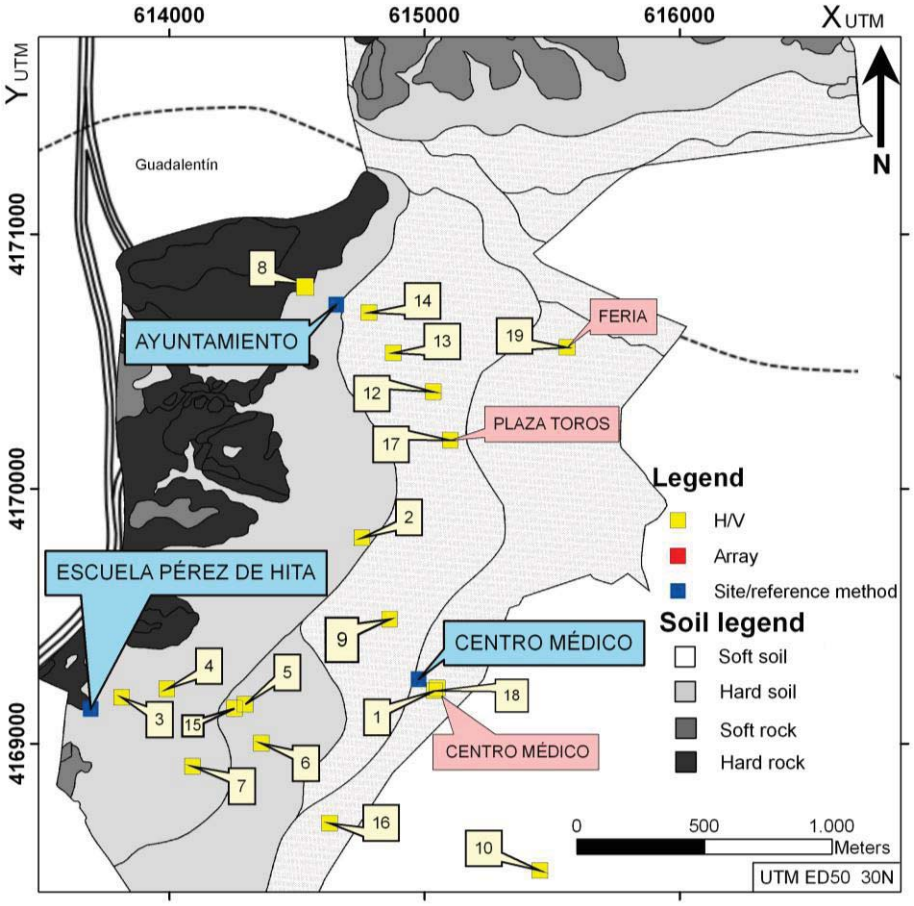

Figure 7. Sketch of geological features under Lorca town (modified from Navarro *et al*. 2012), showing the location of temporary stations (blue) and ambient noise measurement sites: yellow for single stations, red for arrays of sensors. Note that the H/V measurement point #11 is outside the map and that measurement point #8 coincides with LOR station.

POST-SEISMIC INSPECTION SURVEY

In order to characterize the seismic response of soil layers during the Lorca earthquake, a short post-earthquake survey focused on recording both aftershocks and ambient noise was conducted in the town between May 24 and 27 2011.

Single-station ambient noise was recorded in Lorca, both to evaluate the fundamental

frequencies of the different soil types and to try to correlate the possible soil amplifications with observed damage. Measurements were realized along profiles perpendicular to the Guadalentín River to observe the evolution of horizontal-to-vertical (H/V) spectral ratios. Microtremors were also recorded with an array of sensors to obtain estimates of the shear-wave velocity (V_S) in the soil layers. Another purpose was to quantify the soil amplification by applying the site/reference method based on aftershock records. Seismographs were installed at three sites. It was also possible to rely on records from one IGN mobile station located in the delta of the Guadalentín River (IGN, personal communication, 2011). Figure 7 shows the locations of the three seismographs and the sites where point and array seismic noise measurements were acquired.

Fundamental soil frequency

To apply the H/V spectral ratio technique to estimate the fundamental soil frequency (e.g. Bard *et al*. 2005), ambient vibrations were measured at 19 sites in Lorca. Attention was paid to distributing these seismic noise acquisition points along lines perpendicular to the geological structure and near damaged and essential buildings. Measurements were made with a CityShark-II digitizer coupled to a 5s-Lennartz triaxial seismometer. H/V spectral ratios were calculated with the GeoPsy program (Wathelet 2003).

Figure 8 presents H/V spectral ratios for all the considered sites. Half of the experimental H/V ratios show low fundamental soil frequencies, around 1 Hz, which could correspond to the quaternary deposits covering the Guadalentín valley, which is 100-200 meters thick according to a study of ITGE (1992) and Martínez-Díaz *et al*. (2012). Most of the sites located on soft soils show a peak related to the soil fundamental frequency; such peaks are not observed at the majority of sites located on stiff soils. These H/V results are consistent with a generally decreasing predominant frequency from northern and western rock outcrops towards the less consolidated quaternary formations in the central and eastern zones. This feature has been pointed out by Navarro *et al*. (2012).

H/V curves also show low amplitudes and high dispersion, which indicates a succession of lithological formations without strong impedance contrast. The observation of several secondary peaks is associated to vertical heterogeneities in layering. Rock sites having flat H/V curves or high fundamental frequencies (> 10 Hz) are found to the northwest of Lorca, near rock outcrops.

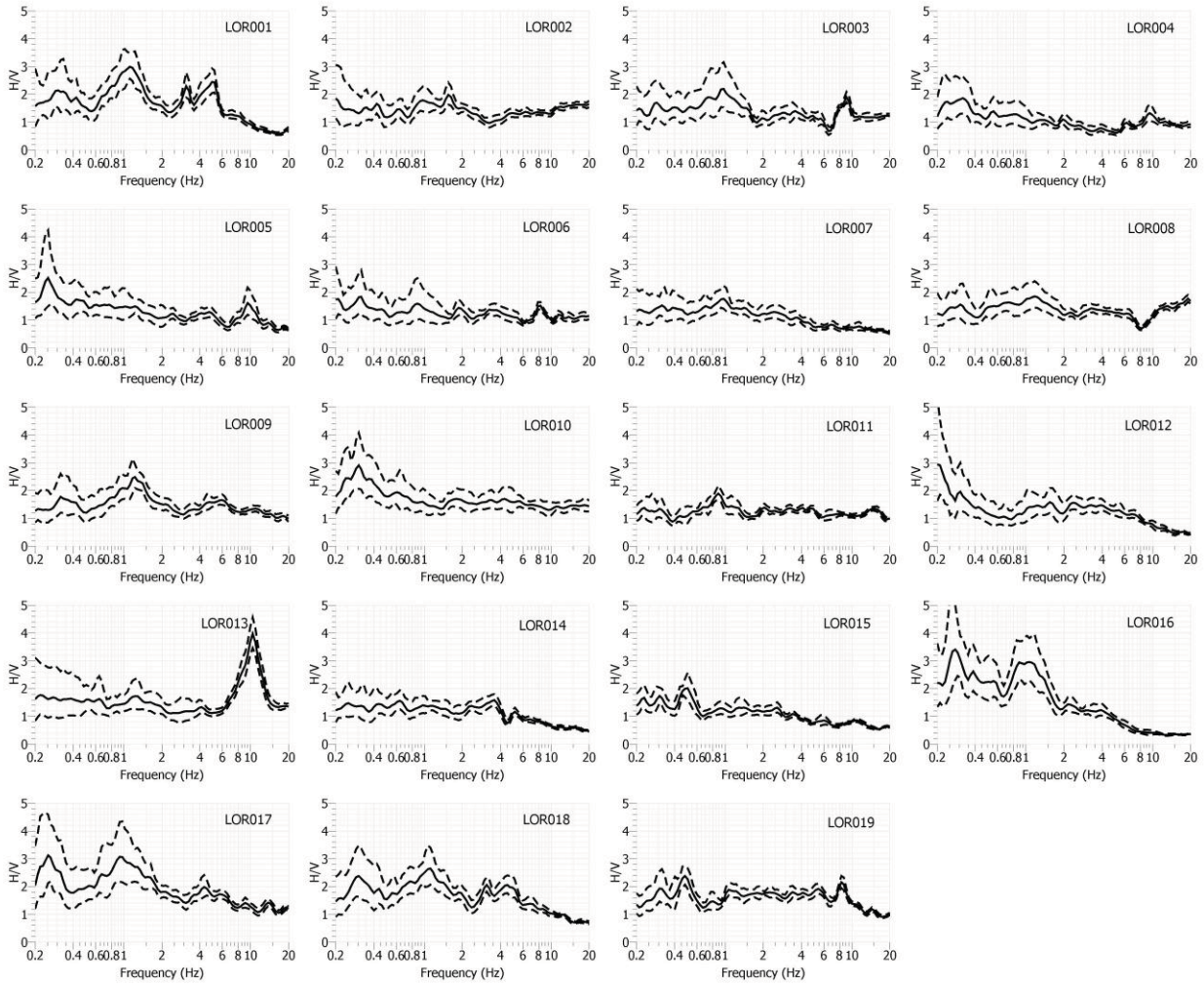

Figure 8. H/V curves obtained on all the experimented sites in Lorca.

Application of the H/V method in Lorca has detected limited soil amplification, which is not surprising. The reliability of the H/V method based on microtremors has been proved for horizontally-layered structures and when a significant impedance contrast exists between sedimentary series and the basement. The presence of specific geological and geometrical configurations may, however, complicate the interpretation of H/V curves. For a set of more than 100 sites, Haghshenas *et al*. (2008) observed a good agreement between the fundamental frequency obtained by the H/V method and from site-to-reference spectral ratios for 81 % of the sites. They mentioned that a significant part of the disagreements correspond to thick, low-frequency, stiff, continental or sites with low impedance contrast. Some locations in the city of Lorca could fulfill these conditions. In some studies conducted in other areas (Bonnefoy-Claudet *et al*. 2007, Belvaux *et al*. 2012), experimental H/V curves have shown similar behavior to those

of Lorca, i.e. low amplification, dispersion and shallow peaks, so that the method has not significantly contributed to effective detection of site amplification. This is notably the case when there are strong lateral variations in velocities, or with the presence of velocity inversions linked to the stratigraphic sequence of multiple soft and stiff layers.

Lorca is located directly over the area of seismic rupture. It is, therefore, possible that the subsoil materials have somehow fragmented and that the mechanical contrasts between them are not strong enough to exhibit clear fundamental frequencies in H/V spectral ratios.

Shear-wave velocity profiles

During the Lorca post-earthquake inspection survey, recordings of ambient noise were acquired in three sites with the array technique (Aki 1957, Wathelet *et al*. 2004). For each site, the purposes were to obtain the vertical profile of shear-wave velocity, and consequently to estimate a soil class according to EC8 and to help define a soil column allowing 1-D seismic soil response modeling. The selected sites are located on soft to stiff soils and close to damaged areas: Bullring (Plaza de toros - LOR17), Medical Center (LOR01) and Feria (LOR19).

Instrumentation consisted of a 24-channels seismometer Summit DMT and eleven 1Hz-vertical geophones Mark L4C. Geophones were distributed along two concentric circles around a central geophone (maximum diameter of 60 m). In addition, experimental H/V curves were calculated at four points of the arrays to validate the hypothesis of a horizontally-stratified soil structure. The H/V curves obtained in different points inside the array deployment have the same shape over the whole frequency band for each array. All the array locations show low soil fundamental frequencies (below 1 Hz).

Figure 9 presents the three vertical shear-wave velocity profiles obtained for the studied sites, with maximum depths between 16 and 60 m. These models have been obtained by applying Frequency – Wave number (FK) and Spatial Autocorrelation (SAPC) methods (Aki 1957) and the GeoPsy inversion process (Wathelet 2003, Wathelet *et al*. 2004). In this case, the superficial soil profiles obtained from array technique cannot be related to the soil fundamental frequency. The observed shallow impedance contrasts are related to higher frequencies, between 3 and 5 Hz, probably the secondary peaks observed in the H/V spectral ratio (Figure 8).

On Figure 9, mean shear-waves velocities over the first 30 meters (V_{S30}) and classification of soil type according to the EC-8 are also given. For the three noise-array sites considered,

superficial soils approximately correspond to EC-8 soil class C (V_{S30} between 180 and 360 m/s). Despite not laying directly on bedrock, these soil formations can present significant impedance contrasts, thereby amplifying seismic waves.

Site/reference soil amplification

Our experimental field survey also measured weak earthquake weak motions. In this case, analyses were carried out using the reference site method, in which spectral ratios of simultaneous records from rock (reference) and sediment stations provides an experimental transfer function for the sediment location (Borcherdt 1970).

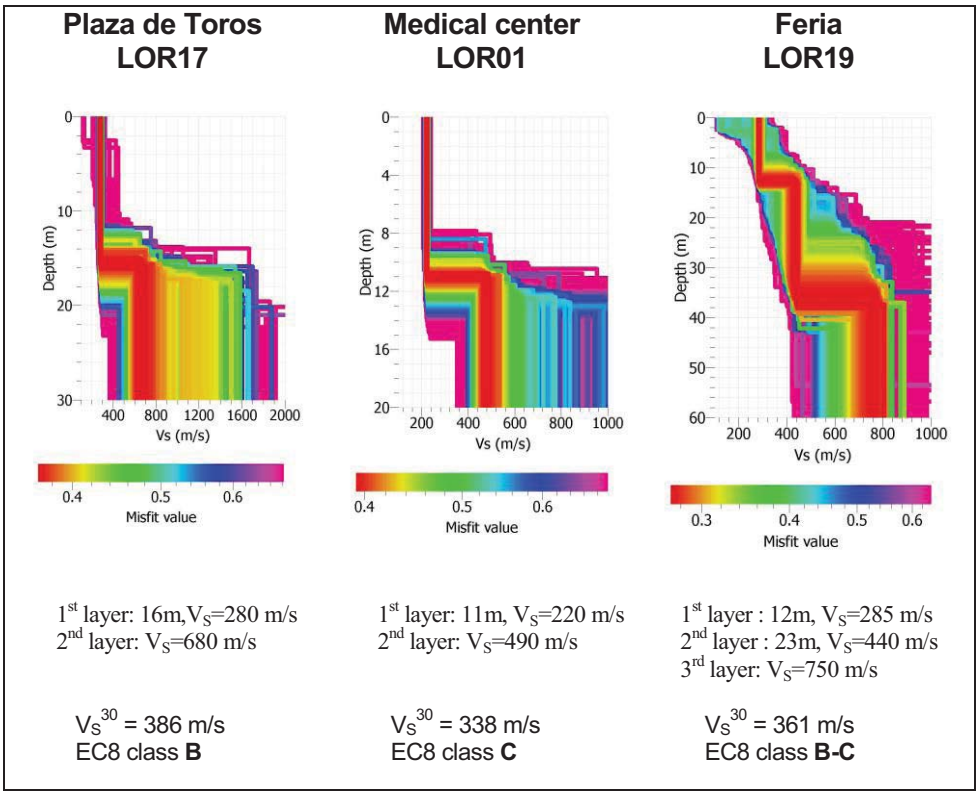

Figure 9. Shear waves profiles versus depth obtained from microtremor array analysis.

In a previous study carried out in Lorca, a local accelerometric network was installed at locations with different soil conditions to characterize soil amplification (Navarro *et al*. 2006). During this study several earthquakes were recorded with magnitudes ranging from 1.9 to 4.7, and depths from 4 to 20 km. This study founded that records obtained at stations on soil have higher amplitudes than the reference site. Amplification factors between 5 and 7 were observed in the transfer functions for periods ranging between 0.1 and 0.3 s.

Between May 24 and 27 2011, three temporary seismic stations were installed to record possible aftershocks on different soil types existing in Lorca (in blue on Figure 7) in order to compute experimental transfer functions. Temporary seismic stations consist of a three-channel Spider datalogger connected to a Lennartz LE-3D 0.2Hz sensor. A complete description can be found in Figueras *et al*. (2012).

During the period when the temporary network was operating, only one aftershock (m_b=1.8) was recorded at two seismic stations (Ayuntamiento and Escuela Pérez de Hita), because the Lorca earthquake was followed by a short aftershock sequence. This aftershock was also recorded on the mobile unit installed by IGN in the Lorca basin (UMV6). Figure 10 shows velocity time-histories and pseudo-velocity response spectrum for the IGN mobile unit (soil class C) and Escuela Pérez de Hita (soil class A). Higher amplitudes for the soil site (factor of two) are observed, thus confirming the ability of unconsolidated materials in the Guadalentín basin to significantly amplify the seismic motion. Since the distance between both stations is not negligible compared to the epicentral distance, the transfer function cannot be accurately estimated.

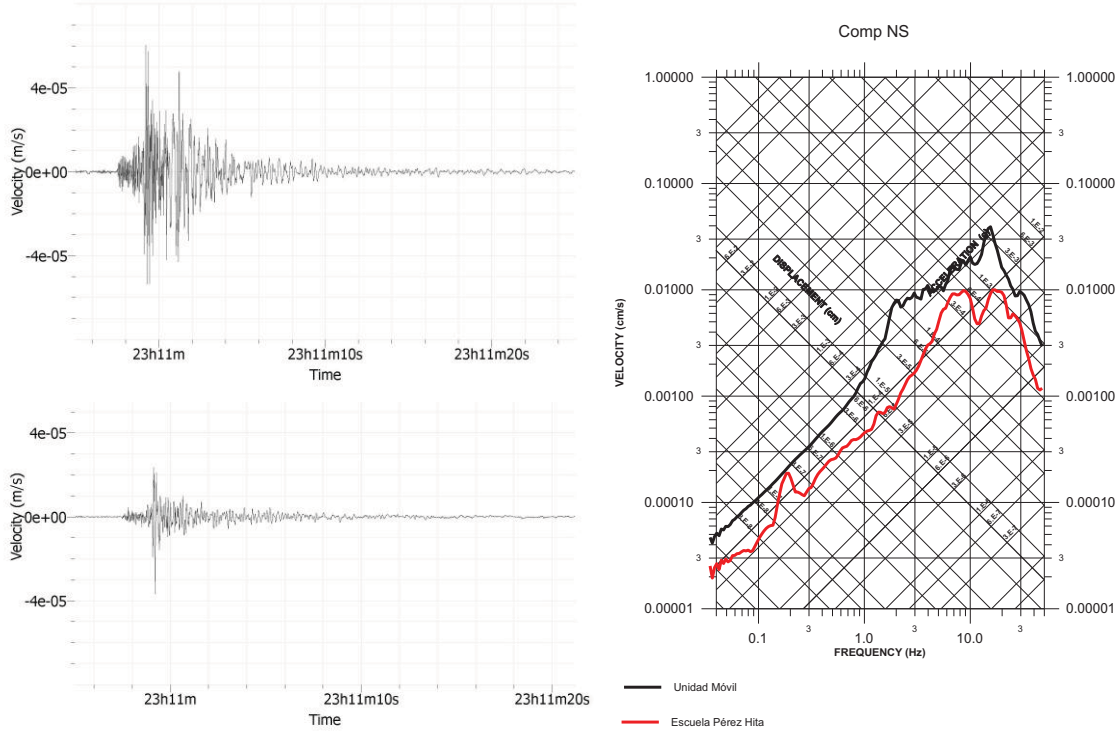

Figure 10. Aftershock velocity time histories recorded on soft soil (top left) compared with rock site (bottom left); and pseudo-velocity response spectra (right).

NUMERICAL ANALYSIS

Different attempts at simplified 1-D soil response analysis were made for several instrumented sites to understand which soil layers have the most significant effect on seismic response. Representative soil columns were defined from experimental V_S profiles and from available geophysical information.

Figueras *et al.* (2012) use a 1-D equivalent linear model intended to analyze sites assumed to be underlain by horizontal infinite layers subjected to vertically-propagating shear waves, with the LOR main shock accelerogram as seismic input. The increase in macroseismic intensity due to the presence of soft soils was assessed. Conclusions might indicate that the intensity VII estimated by the IGN as an average value for the whole of Lorca, might change locally between VI-VII for rock sites and VII-VIII for soil type C sites.

Modeling based on surface-wave propagation was also made for selected soil columns. One example shown here is for LOR01 (Medical Center), where soil amplification is the most marked among the three passive array sites. The point is located inside a building complex damaged during the Lorca earthquake, close to a medical center. The H/V curve presents small peaks at 1.2, 3.2 and 5 Hz (Figure 11). Synthetic H/V curves were generated using the H/V modeling routine for stratigraphic analyses implemented in the *Grilla* software. This code is based on the simulation of the surface-wave field (Rayleigh and Love) in plane-parallel multi-layered systems, according to the theory described by Aki (1964) and Ben-Menahem and Singh (1981). Details on the comparison between the H/V modeling technique code implemented in *Grilla* and the passive array technique are published in Castellaro and Mulargia (2009).

For LOR01, Figure 11 shows the experimental H/V curve (in red), the synthetic curve (in blue) and the V_S profile used to run the model. In all layers V_P has been derived from V_S using a Poisson modulus of 0.31. Multiple resonance peaks are found on this experimental H/V curve. The 1.1-1.2 Hz peak seems to be related to a thick formation (about a hundred meters deep) with a mean shear-wave velocity of around 600 m/s, likely formed of sediment filling the Guadalentín basin. The model failed to match one of the higher frequency peaks, which informs us about a superficial layer of at least ten meters of soft material (probably alluvial deposits) having a V_S of 200-250 m/s. These characteristics reflect the complexity of the shallow geological structure under Lorca.

Our knowledge on the prevailing geological formations constituting the Lorca subsurface is partial and almost no information on the geotechnical characteristics of these soil sequences was available. Although there remain many uncertainties in evaluating soil properties, it is verified here that Quaternary formations of variable thickness led to ground-motion amplification at specific locations during the Lorca earthquake. It is advisable that future work addresses basin effects through refined 2-D analysis.

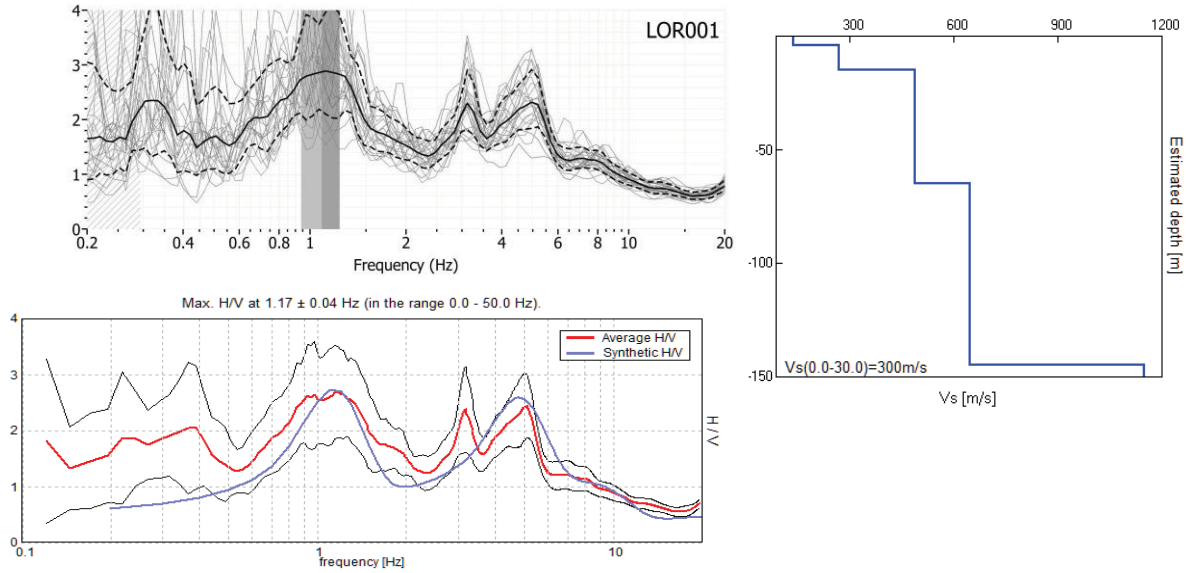

Figure 11. H/V modeling and resulting stratigraphic soil profile for LOR01 site. Experimental H/V curves obtained through *GeoPsy* (top left) and *Grilla* (in red on bottom left) software, synthetic H/V curve (in blue on bottom left), V_S profile (right).

CONCLUSIONS

Acelerograms obtained in the Murcia region during the Lorca earthquakes of May, 2011 have provided the Spanish database with some truly 'strong' motions. In particular, the records obtained in Lorca have contributed much to near-field seismology. They demonstrate rupture directivity, with a larger N30ºW component than the N60ºE one, and a pulse with a period of about 0.4s. This pulse constitutes the major difference in spectral shape with regard to the EC-8 type 2 response spectrum for a site class A. Through the combination of high accelerations and short duration of strong motions, rupture directivity effects have certainly played a role in the specificity of observed damage to Lorca's structures.

From 19 ambient seismic noise measurements, the soil fundamental frequencies obtained in Lorca seem to be low, half of them are around 1 Hz. These frequencies correspond to soil

deposits with a thickness of several tens of meters. On the other hand, no marked contrasts between soil types have been observed with the H/V spectral ratio technique; the method seems inefficient in detecting soil amplification in this case. Due to the proximity of the Alhama de Murcia fault, the geometry and nature of sedimentary bodies are probably altered by the fault activity. It is, therefore, possible that the impedance contrasts between subsurface materials are not strong enough to exhibit clear fundamental frequencies in the H/V spectral ratios.

The results obtained with the array technique and from the data recorded by the temporary three-component seismographs indicate that the presence of superficial soil layers with low V_S (EC8 soil class C) might have amplified the seismic waves during the Lorca earthquake. However, these results are not detailed enough to correlate these possible effects with observed heterogeneities in damage in the town.

These events provide an opportunity to study and analyze, among other areas, the role that microzonation, urban planning and design could play in effectively mitigating earthquake risk in the urban areas of Spain and adjacent countries.

Acknowledgements

The Municipal Police of the city of Lorca is gratefully acknowledged for having supported the field activities during the three days when measurements were made in the town. The post-earthquake mission was supported by the Spanish Association of Earthquake Engineering (AEIS) and the AFPS (French Association of Earthquake Engineering). We acknowledge the IGN (National Geographic Institute) for providing their data. The work presented in this paper was carried out with funding from IGC and BRGM, who are thanked for their support. Thanks are also due to John Douglas for reading and improving the manuscript. Finally we thank the two anonymous reviewers for their careful revisions of the manuscript and for their contributions to improve the work.

REFERENCES

AFPS, 2011. *Le seisme de Lorca (Espagne) du 11 mai 2011*. Rapport de mission de l'Association Française de Génie Parasismique, Décembre 2011, 151p.

Aki, K., 1957. Space and time spectra of stationary stochastic waves, with special reference to microtremors, *Bull. Earth. Res. Inst.* **35**, 415-456.

Aki, K., 1964. A note on the use of microseisms in determining the shallow structures of the earth's crust. *Geophysics* **29**, 665-666.

Akkar, S., and Bommer, J., 2010. Empirical Equations for the Prediction of PGA, PGV, and Spectral Accelerations in Europe, the Mediterranean Region, and the Middle East. *Seismological Research Letters* **81**, 195-206.

Bard, P.-Y., and the SESAME team, 2005. *SESAME European research project (WP12 - D23.12). Guidelines for the implementation of the H/V spectral ratio technique on ambient vibration measurements, processing and interpretation*. 62p. Available at http://sesame-fp5.obs.ujf-grenoble.fr.

Ben-Menahem, A., and Singh, S.J., 1981. *Seismic Waves and Sources*, Springer-Verlag, New York.

Belvaux, M., Roullé, A., Auclair, S., Vanoudheusden, E., and Barras, A.-V., 2012. Limites des methodes de caracterisation des effets de site dans les microzonages sismiques. *Journées Nationales de Géotechnique et de Géologie de l'Ingénieur JNGG2012* – Bordeaux 4-6 Juillet.

Bommer, J.J., Georgallides, G., and Tromans, I.J., 2001. Is there a near-field for small-to-moderate magnitude earthquakes? *Journal of Earthquake Engineering* **5**, 395-423.

Bonnefoy-Claudet S., Baize, S., Bonolla, F., Berge-Thierry, C., Campos, J., Pasten, C., Verdugo, J., and Volant, Ph., 2007. Comment caractériser les effets de site des structures complexes à partir du bruit ambiant. Application au bassin de Santiago du Chili. *7ème Colloque National AFPS*, Ecole Centrale Paris, France, 4-6 Juillet 2007.

Borcherdt, R.D., 1970. Effects of local geology on ground motion near San Francisco Bay, *Bull. Seismol. Soc. Am.* **60**, 29-61.

Bousquet, J.-C., 1979. Quaternary strike-slip faults in southeastern Spain, *Tectonophysics* **52**, 277-286.

Buforn, E., Benito, B., Sanzde Galdeano, C., del Fresno, C., Muñoz, D., and Rodríguez, I., 2005. Study of the damaging earthquakes of 1911, 1999, and 2002 in the Murcia, Southeastern Spain region: seismotectonic and seismic-risk implications, *Bull. Seismol. Soc. Am*. **95**, 549-567.

Buforn, E., Cesca, S., Goded, T., del Fresno, C., and Muñoz, D., 2006. The Bullas (Murcia, SE Spain) earthquake, 29 January 2005. *Journal of Seismology* **10**, 65-72.

Cabañas, L., Benito, B., Cabañas, C, López, M., Gómez, P., Jiménez, M. E., and Álvarez, S., 1999. Banco de datos de movimiento fuerte del suelo MFS. Aplicaciones. pp 113-139 of Complutense (ed), *Física de la Tierra*, vol. 11. In Spanish with English abstract.

Cabañas, L., Alcalde, J. M., Carreño, E., and J.B. Bravo, 2013. Characteristics of observed strong motion accelerograms from the 2011 Lorca (Spain). *Bulletin of Earthquake Engineering*. DOI 10.1007/s10518-013-9501-0. Springer, Netherlands.

Castellaro, S., and Mulargia, F., 2009. V_{S30} Estimates Using Constrained H/V Measurements. *Bull. Seismol. Soc. Am.* **99**, 761-773.

Chai, J., Loh, C., and Chen, C., 2000. Consideration of the near-fault effect on seismic desing code for sites near the Chelungpu fault. *Journal of the Chinese Institute of Engineers* **23**, 447-454.

EC-8 CEN, 2004. *Comité Européen de Normalisation, Eurocode-8: Design of Structures for Earthquake Resistance*. Part 1, Brussels, 229 pp. Doc CEN/TC250/SC8/N335, January.

EPRI, 1991. *Standardization of the Cumulative Absolute Velocity*, Report No. EPRI TR-100082-T2, Palo Alto, California.

EPRI, 2006. *Program on Technology Innovation: Use of Cumulative Absolute Velocity (CAV) in Determining Effects of Small Magnitude Earthquakes on Seismic Hazard Analysis*. Technical Report.

Figueras, S., Macau, A., Peix, M., Belvaux, M., Benjumea, B., Gabàs, A., Susagna, T., and Goula, X., 2012. Caracterización de efectos sísmicos locales en la ciudad de Lorca. *Física de la Tierra* **24**, 235-254.

Frontera, T., Concha, A., Blanco, P., Echeverria A., Goula, X., Arbiol, R., Khazaradze, G., Pérez, F., and Suriñach E., 2012. DInSAR Coseismic Deformation of the May 2011 Mw 5.1 Lorca Earthquake (southeastern Spain). *Solid Earth* **3**, 111-119.

Gaspar-Escribano, J.M., Benito, B., and García-Mayordomo, J., 2008. Hazard-consistent response spectra in the Region of Murcia (Southeast Spain): comparison to earthquake-resistant provisions, *Bulletin of Earthquake Engineering* **6**, 179-196, doi:10.1007/s10518-007-9051-4.

Haghshenas, E., Bard, P.Y., Theodulidis, N., and SESAME WP04 Team, 2008. Empirical evaluation of microtremor H/V spectral ratio. *Bulletin of Earthquake Engineering* **6**, 75-108.

IGC, 2011. *El Terremoto de Lorca, España, 11 de mayo de 2011: Informe técnico de inspección y de los trabajos de campo realizados*. IGC, UPC, AEIS. Monografía técnica nº 3, Barcelona,·86 pp.

IGN, 2011. *Informe del sismo de Lorca del 11 de Mayo 2011*. Madrid, Julio 2011, http://www.ign.es/ign/resources/sismologia/Lorca.pdf

IGME, 2011. *Informe geológico preliminar del terremoto de Lorca del 11 de mayo del año 2011, 5.1 M_w*. Instituto Geológico y Minero de España, Grupo de Tectónica Activa, Paleosismicidad y Riesgos Asociados de la Universidad Complutense de Madrid (UCM), Universidad Autónoma de Madrid (UAM) y la Universidad Rey Juan Carlos de Madrid (URJC).

ITGE, 1992. *Estudio de peligrosidad y vulnerabilidad sísmica en Lorca y su término municipal*, Instituto Tecnológico y Geominero de España (ITGE), Empresa de Estudios Geológicos - Geotécnicos (GEONOC).

Lopez-Comino, J.A., Mancilla, F., Morales, J., and Stich, D., 2012. Rupture directivity of the 2011, M_w 5.2 Lorca earthquake (Spain). *Geophysical Research Letters* **39**, L03301, http://dx.doi.org/10.1029/2011GL050498.

Martínez-Díaz, J.J., 2002. Stress field variety related to fault interaction in a reverse oblique-slip fault: the Alhama de Murcia Fault, Betic Cordillera, Spain. *Tectonophysics* **356**, 291-305.

Martínez-Díaz, J.J., Masana, E., Hernández-Enrile, J.L., and Santanach, P., 2003. Effects of repeated paleoearthquakes on the Alhama de Murcia Fault (Betic Cordillera, Spain) on the Quaternary evolution of an alluvial fan system, *Annals of Geophysics* **46**, 775-791.

Martínez-Díaz, J.J., Bejar-Pizarro, M., Álvarez-Gómez, J.A.,c, Mancilla, F.L., Stich, D., Herrera, G., and Morales, J., 2012. Tectonic and seismic implications of an intersegment rupture. The damaging May 11th 2011 M_w 5.2 Lorca, Spain, earthquake. *Tectonophysics*. doi:10.1016/j.tecto.2012.04.010.

Martínez-Solares, J.M., and Mezcua, J., 2002. Catálogo sísmico de la Península Ibérica (880 a.C.-1900), *Monografía núm.* **18**, Subdirección General de Geodesia y Geofísica, Instituto Geográfico Nacional, Madrid (in Spanish).

Masana, E., Martínez-Díaz, J.J., Hernández-Enrile, J.L., and Santanach, P., 2004. The Alhama de Murcia fault (SE Spain), a seismogenic fault in a diffuse plate boundary: Seismotectonic implications for the Ibero-Magrebian region, *Journal of Geophysical Research* **109**, B01301, doi:10.1029/2002JB002359.

Mezcua, J., Garcia Blanco, R.M., and Rueda, J., 2008. On the strong ground motion attenuation in Spain. *Bull. Seismol. Soc. Am.* **98**, 1343-1353.

Muñoz, D., and Udías, A., 1991. Three large historical earthquakes in southeastern Spain. In: *Seismicity, Seismotectonics and Seismic Risk of the Ibero Maghrebian Region*, Instituto Geográfico Nacional, Madrid, 175-182.

Musson, R.M.W., Grünthal, G., and Stucchi, M., 2010. The comparison of macroseismic intensity scales, *Journal of Seismology* **14**, 413-428. DOI 10.1007/s10950-009-9172-0.

Navarro, M., García-Jerez, J.A., Vidal, F., Enomoto, T., Pérez-Ruiz, J.A., Alcalá, F.J., Luzón, F., Yamamoto, T., and Iwatate, T., 2006. Características del movimiento del suelo a partir de medidas de vibración ambiental y registros de aceleración. *5ª Asamblea Hispano-Portuguesa de Geodesia y Geofísica*. Sevilla.

Navarro, M., García-Jerez, J.A., Alcalá, F.J., Vidal, F., Enomoto, T., Luzón, F., and Creus, C., 2008. V_S^{30} Structure of Lorca town (SE Spain) from Ambient Noise Array Observations. *31st General Assembly of the European Seismological Commission ESC*, Hersonissos, Crete, Greece, 7-12 September 2008.

Navarro, M., García-Jerez, J.A., Alcalá, F.J., Vidal, F., Aranda, C., and Enomoto, T., 2012. Analysis of site effects, building response and damage distribution observed due to the 2011 Lorca, Spain, Earthquake. *15th World Conference of Earthquake Engineering 15WCEE*, Lisboa, Portugal, 24-28 September 2012.

NCSE-2002, 2002. *Norma de Construccion Sismorresistente NCSE-2002*, BOE 244, 11 Octubre 2002.

Rueda, J., Mezcua, J., and García Blanco, RM., 2011. Directivity effects of the May 11, 2011 Lorca (Spain) Mw=5.1 earthquake. *AGU Fall meeting*, San Francisco, California, USA, 5-9 December.

Santoyo, M.A., 2013. Finite fault analysis and near field dynamic strains and rotations due to the 11/05/2011 (M_w5.5) Lorca earthquake, South-Eastern Spain. *Bulletin of Earthquake Engineering.* DOI 10.1007/s10518-013+9492-X. Springer, Netherlands.

Somerville, P.G., Smith, N.F., Graves, R.W., and Abrahamson, N.A., 1997. Modification of empirical strong ground motion attenuation relations to include the amplitude and duration effects of rupture directivity, *Seismological Research Letters* **68**, 199-222.

Somerville, P.G., 2003. Magnitude scaling of the near fault rupture directivity pulse. *Physics of the Earth and Planetary Interiors* **137**, 201-212.

Souriau, A., 2006. Quantifying felt events: A joint analysis of intensities, accelerations and dominant frequencies. *Journal of Seismology* **10**, 23-38. DOI: 10.1007/s10950-006-2843-1.

Susagna, T., Cabañas, L., Goula, X., Alcalde, J.M., and Belvaux, M., 2012. Análisis de los parámetros de los acelerogramas registrados en los seísmos de Lorca, de interés para la Ingeniería. *Física de la Tierra* **24**, 213-234.

Tapia, M., Susagna, T., and Goula, X., 2007. Curvas predictivas del movimiento del suelo en el oeste del Mediterráneo. *3er Congreso Nacional de Ingeniería Sísmica*, 8-11 Mayo 2007, Girona. CD-Rom 17pp.

Uniform Building Code, 1997. *International Conference of Building Officials*, Wittier, Ca.

Wald, D., Quitoriano, V., Heaton, T., and Kanamori, H., 1999. Relationships between peak ground acceleration, peak ground velocity and modified Mercalli intensity in California. *Earthquake Spectra* **15**, 557-564.

Wathelet, M., 2003. *Report on the inversion of velocity profile and version0 of the inversion software SESAME* Report D14.07.

Wathelet, M., Jongmans, D., and Ohrnberger, M., 2004. Surface wave inversion using a direct search algorithm and its application to ambient vibration measurements, *EGU first general assembly*, Nice, France.